

Phase transitions in a square Ising model with exchange and dipole interactions

E. Rastelli,* S. Regina, and A. Tassi

Dipartimento di Fisica, Università di Parma, Parco Area delle Scienze 7/A, 43100 Parma, Italy

(Received 8 February 2006; revised manuscript received 17 March 2006; published 17 April 2006)

Competition between dipole and nearest neighbor exchange interaction in the square Ising model is responsible for the occurrence of antiferromagnetic and striped configurations the width of which, h , increases at increasing J/g , where J and g are the strength of the exchange and the dipole interaction, respectively. Extensive Monte Carlo simulations and finite-size scaling analysis are performed to investigate the nature of the order-disorder phase transition for selected values of J/g supporting the antiferromagnetic configuration and the striped configurations with $h=1, 2, 3, 4$. Both continuous and first order phase transitions are recognized.

DOI: [10.1103/PhysRevB.73.144418](https://doi.org/10.1103/PhysRevB.73.144418)

PACS number(s): 75.10.Hk, 75.40.Cx, 75.40.Mg

I. INTRODUCTION

Frustration caused by competing interactions supports complex spin configurations and rich phase diagrams are found even though any single interaction is simple in nature.

A famous example is the anisotropic next nearest neighbor Ising (ANNNI) model¹ in two and three dimensions where the competition between the nearest neighbor (NN) interaction J_1 and the next nearest neighbor (NNN) interaction J_2 is restricted to one direction (i.e., the x axis) of a square or a simple cubic lattice. The phase diagram of the three-dimensional (3D) ANNNI model is divided in three regions of the ($\kappa = -J_2/J_1, k_B T/J_1$) plane corresponding to ferromagnetic ($\kappa < \frac{1}{2}$), sinusoidal ($\kappa > \frac{1}{2}$), and paramagnetic phase [$T > T_c(\kappa)$].

The ground state of the sinusoidal phase consists of a stacking of two ferromagnetic planes of spins up followed by two ferromagnetic planes of spins down and so on ($\langle\langle 2 \rangle\rangle$ phase). Mean field theory, high temperature series expansion, and Monte Carlo (MC) simulations were developed in order to draw the transition lines of the phase diagram and to investigate the main features of the sinusoidal phase.²

The Fourier analysis of the magnetization obtained by MC simulation for $\kappa=0.6$ pointed out that the wave vector characterizing the ground state configuration ($q = \pi/2$) does not change up to $T \approx 0.8T_c$ then it falls off to a critical value $q_c \approx 1.2$ between 0.8 and $0.9T_c$. The value of q_c no longer changes up to the critical temperature.²

In the two-dimensional (2D) ANNNI model the scenario is more complex because a modulated “floating incommensurate” (Kosterlitz-Thoulesslike³) phase intervenes between the low temperature ordered phase and the high temperature paramagnetic one.⁴ The ground state configuration ($\langle\langle 2 \rangle\rangle$ phase) is a striped configuration where two rows (columns) of spins down alternate with two rows (columns) of spins up. No change of the wave vector was observed in the ordered phase.

A 2D isotropic Ising model with competing NN J_1 and (diagonal) NNN J_2 exchange interactions was carefully studied by MC simulation and critical exponents out of the Ising universality class were found.⁵ An explanation was tried based on the possible mapping of this model into the 2D

planar model with a fourfold breaking symmetry field for which nonuniversal critical indices were obtained by renormalization group calculation⁶ and confirmed by MC simulation.⁷

The square Ising model with the spins pointing out of the plane, coupled by NN exchange interaction J and dipole interaction g , shows a variety of ground state configurations⁸ depending on the ratio J/g . Indeed for $J=0$ (pure dipole interaction) the ground state corresponds to an antiferromagnetic (AF) Néel configuration. As the ratio J/g increases, the ground state is characterized by “striped” configurations with alternating rows (columns) of spins up and down of width h , where h increases with J/g . This model is suitable to catch the qualitative features of the spin configurations observed in ultrathin films of magnetic atoms on metal substrates.⁹

As for the nature of the order-disorder transition, not well established conclusions exist. For $J=0$ a continuous phase transition with critical exponents of the 2D NN Ising universality class was not excluded on the basis of MC simulations.¹⁰ On the other hand, a first order phase transition was clearly¹¹ indicated for $J/g=4$ ($h=2$). The first order nature of the order-disorder transition was extended to any striped configuration by a self-consistent Hartree-Fock (SCHF) approximation applied to the continuous version of the Hamiltonian model.¹¹ The SCHF approximation was previously introduced for a model with an excitation energy spectrum showing a rotonlike minimum¹² and subsequently applied to a 3D Ising model with ferromagnetic NN coupling and long range Coulomb interaction.¹³ Also for this model a first order phase transition was found for any value of the Coulomb interaction Q , including $Q=0$. For $Q=0$ the model reduces to the 3D NN Ising model for which the transition is continuous. The conclusion could be that the mean field approximation leads always to continuous phase transitions; the fluctuations accounted for by the SCHF approximation drive always the transition to first order.

Since the order of the transition is a debated question we have performed extensive MC simulations for selected values of $J/g=0, 1.7, 3.4, 5, 6$, for which the low temperature phase corresponds to the AF configuration and to the striped configurations with $h=1, 2, 3, 4$, respectively. Continuous order-disorder phase transitions are found for the AF phase

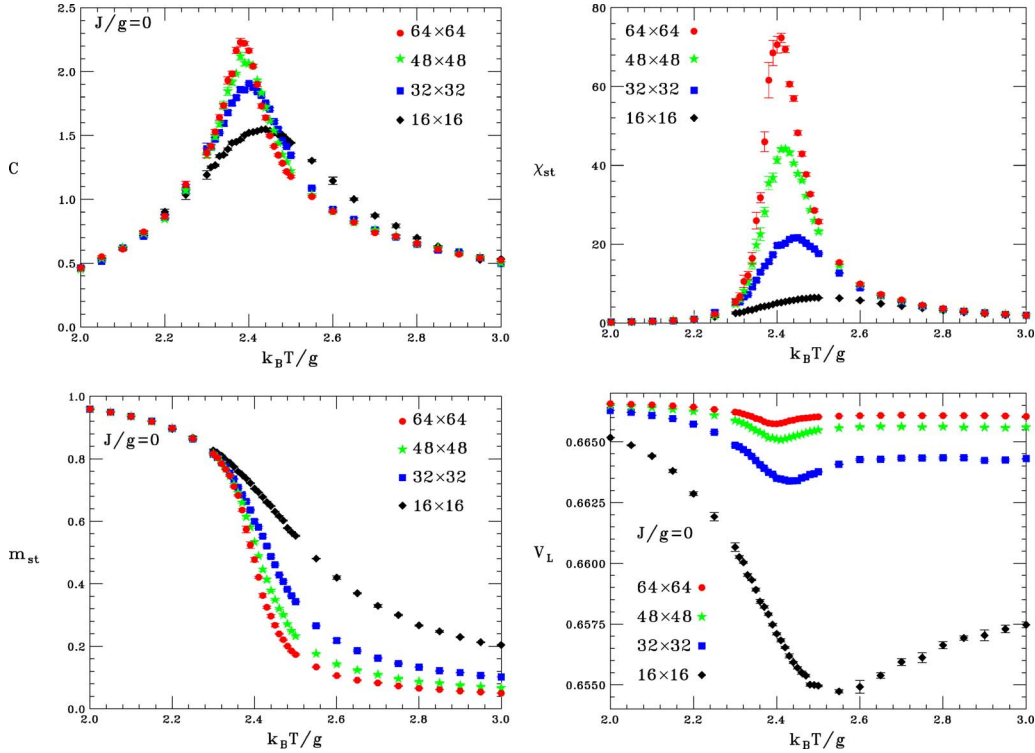


FIG. 1. (Color online) Thermodynamic quantities for $J/g=0$ (AF phase): (a) specific heat C , (b) staggered magnetization m_{st} , (c) staggered susceptibility χ_{st} , (d) fourth order energy cumulant V_L vs temperature for $L=16$ (diamonds), $L=32$ (squares), $L=48$ (stars), and $L=64$ (circles).

and for the striped configurations with $h=1$ and $h=4$. A clear first order phase transition occurs for $h=2$ while for $h=3$ the transition appears to be weakly first order.

For all values of J/g investigated no change in the wave vector characterizing the low temperature spin configuration was recorded and no intermediate Kosterlitz-Thoulesslike phase between the low temperature ordered phase and the paramagnetic one was singled out.

The critical exponents for the AF phase with $J=0$ (pure dipole interaction) are consistent with the critical exponents of the 2D Ising model with NN interaction in agreement with the previous suggestion.¹⁰ The order-disorder phase transition for the striped configuration for $J/g=1.7$ ($h=1$) is continuous but a careful examination of the finite-size scaling behavior of the staggered susceptibility, the order parameter, and the specific heat suggests critical exponents out of any known universality class. Indeed we find $\nu=1$, $\gamma=1.75$ (as for the 2D NN Ising model) but $\beta=0.08$. The value of $\alpha=0.09$ obtained by the scaling law $\gamma+2\beta=2-\alpha$ compares favorably with the finite-size scaling analysis of the specific heat. Also the hyperscaling law $d\nu=2-\alpha$ is satisfied within the error bars.

For $J/g=3.4$ ($h=2$) the transition is unambiguously first order, while for $J/g=5$ ($h=3$) it seems to be only weakly first order even though the numerical uncertainty does not allow a definite conclusion. Finally, for $J/g=6$ ($h=4$) the transition is continuous with critical exponents undistinguishable from the NN Ising ones. Obviously, for $J/g \rightarrow \infty$ critical exponents and critical amplitudes of the 2D NN Ising model are recovered.

II. MONTE CARLO SIMULATION

The Hamiltonian of the model is

$$\mathcal{H} = -J \sum_{\langle i,j \rangle} \sigma_i \sigma_j + g \sum_{i \neq j} \frac{1}{r_{ij}^3} \sigma_i \sigma_j, \quad (1)$$

where the first sum is restricted to distinct pairs of NN spins and a ferromagnetic interaction $J > 0$ is assumed; in the second sum i and j run over all the sites of a square lattice $L \times L$. The spins $\sigma_i = \pm 1$ are supposed to be aligned out-of-plane. The ground state configurations are AF for $0 < J/g < 0.86$; striped configurations of width $h=1$ for $0.86 < J/g < 2.52$, of width $h=2$ for $2.52 < J/g < 4.35$, of width $h=3$ for $4.35 < J/g < 5.63$, of width $h=4$ for $5.63 < J/g < 6.92$, and so on.^{8,14}

We have performed extensive MC simulations for $J/g=0$ (AF phase), $J/g=1.7$ ($h=1$), $J/g=3.4$ ($h=2$), $J/g=5$ ($h=3$), $J/g=6$ ($h=4$), for lattice sizes $L=16, 24, 32, 48, 60, 64, 96$ with periodic boundary conditions. Note that the lattice sizes 24, 48, 60, 96 are convenient to describe lattices in which stripes of width $h=3$ occur in order to satisfy the periodic boundary conditions.

Eight independent MC runs of 10^5 MC steps per spin (MCS) have been performed at each temperature. The final configuration of the previous temperature is assumed as the starting configuration for the next temperature disregarding 10 000 MCS for thermalization. Because of the long range nature of the dipole interactions the computing time is rapidly increasing. For example, for a lattice size $L=96$ each data point takes more than one day of computing time. For

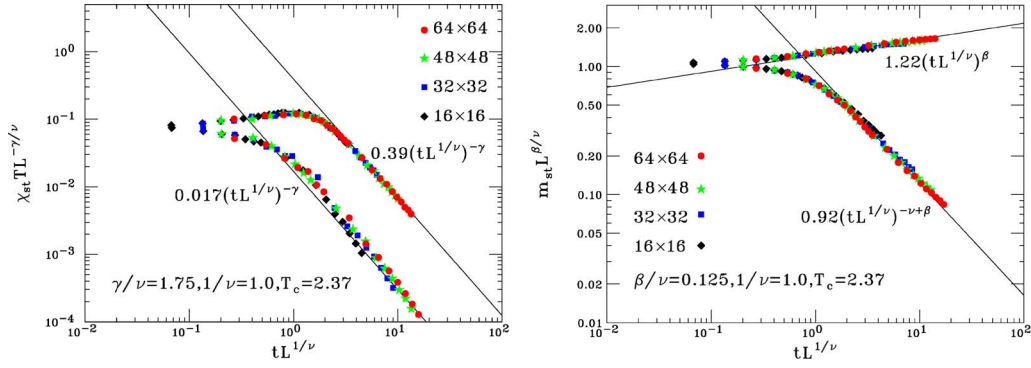


FIG. 2. (Color online) Finite-size scaling functions for $J/g=0$: (a) staggered susceptibility χ_{st} , (b) staggered magnetization m_{st} for $L=16$ (diamonds), $L=32$ (squares), $L=48$ (stars), and $L=64$ (circles).

any MC simulation we evaluate the specific heat

$$C = \frac{\langle \mathcal{H}^2 \rangle - \langle \mathcal{H} \rangle^2}{L^2 k_B T^2}, \quad (2)$$

the internal energy per spin

$$E = \frac{\langle \mathcal{H} \rangle}{L^2}, \quad (3)$$

the fourth-order energy cumulant¹⁵

$$V_L = 1 - \frac{\langle \mathcal{H}^4 \rangle}{3\langle \mathcal{H}^2 \rangle^2}, \quad (4)$$

the order parameter¹⁶

$$O_{hw} = \left\langle \left| \frac{n_h - n_v}{n_h + n_v} \right| \right\rangle, \quad (5)$$

where n_h (n_v) is the number of horizontal (vertical) pairs of NN antiparallel spins. Note that this parameter is zero in the AF phase where it is replaced by the conventional staggered magnetization

$$m_{st} = \frac{1}{L^2} \left\langle \left| \sum_{i \in 1} \sigma_i - \sum_{j \in 2} \sigma_j \right| \right\rangle, \quad (6)$$

where labels 1 and 2 refer to the two sublattices of the antiferromagnetic configuration. For the $h=1$ striped phase we have evaluated the staggered magnetization introduced by Binder and Landau to study the Ising model with NN and NNN interactions,⁵ that is

$$m_{st} = \langle [(M_{st}^1)^2 + (M_{st}^2)^2]^{1/2} \rangle, \quad (7)$$

where

$$M_{st}^1 = [M_1 + M_2 - (M_3 + M_4)]/4 \quad (8)$$

and

$$M_{st}^2 = [M_1 + M_4 - (M_2 + M_3)]/4, \quad (9)$$

where $M_\lambda = 4/L^2 \sum_{i \in \lambda} \langle \sigma_i \rangle$ ($\lambda=1,2,3,4$) are the four sublattice magnetizations appropriate to describe the configuration with alternating rows (columns) of spins up and down. We have also investigated the staggered susceptibility

$$\chi_{st} = \frac{L^2}{k_B T} (\langle m_{st}^2 \rangle - \langle m_{st} \rangle^2) \quad (10)$$

for the AF and striped configuration with $h=1$.

A careful investigation of the lattice size dependence of the MC data was performed in order to recognize whether the order-disorder phase transition is continuous or first order. For continuous transitions the finite-size scaling theory makes it possible to evaluate the critical temperature and to predict the critical exponents.

The finite-size scaling theory is based on the assumption that near the transition the singular part of the free energy can be written as a product of $L^{-(2\beta+\gamma)/\nu}$ times a ‘‘scaling’’ function of $x=L^{1/\nu}|1-T/T_c|$, where $T_c=T_c(\infty)$ is the infinite-lattice critical temperature. This assumption leads to the relationships¹⁷

$$\begin{aligned} m &= L^{-\beta/\nu} X^0(x), \\ \chi T &= L^{\gamma/\nu} Y^0(x), \\ C &= L^{\alpha/\nu} Z^0(x), \end{aligned} \quad (11)$$

where m , χ , and C are the order parameter, susceptibility, and specific heat, respectively. The functions $X^0(x)$, $Y^0(x)$, $Z^0(x)$ are ‘‘universal’’ functions of the variable x . Equations (11) are used by varying simultaneously the critical temperature and the critical exponents until the curves obtained from MC simulation for different lattice size fall on a single ‘‘universal’’ curve. For large x (i.e., $|1-T/T_c| \ll 1$ but $L \rightarrow \infty$), Eqs. (11) are expected to show a power law behavior

$$\begin{aligned} X^0(x) &\rightarrow Bx^\beta, \\ Y^0(x) &\rightarrow C^\pm x^{-\gamma}, \\ Z^0(x) &\rightarrow A^\pm x^{-\alpha}, \end{aligned} \quad (12)$$

in order to ensure the correct asymptotic behavior of the correspondent thermodynamic quantities in the thermodynamic limit. B , C^\pm , and A^\pm are the critical amplitudes (C^+ and A^+ for $T > T_c$ and C^- and A^- for $T < T_c$) of the infinite-lattice model.

Finally, the structure factor

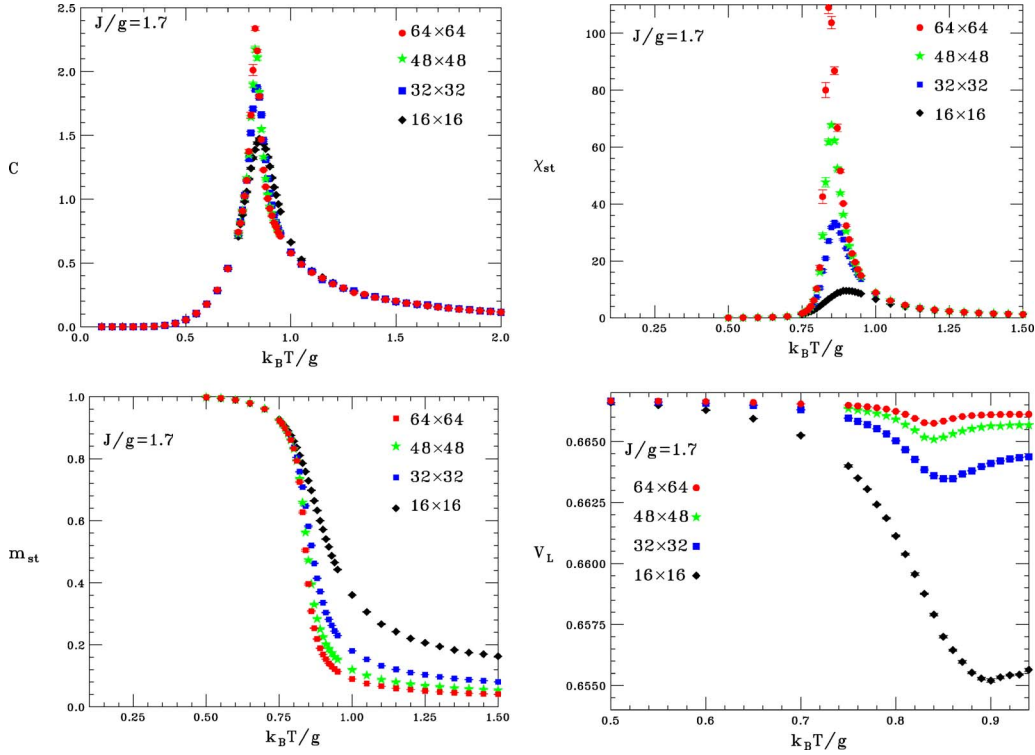


FIG. 3. (Color online) Thermodynamic quantities for $J/g=1.7$ ($h=1$): (a) specific heat C , (b) staggered magnetization m_{st} , (c) staggered susceptibility χ_{st} , (d) fourth order energy cumulant V_L vs temperature for $L=16$ (diamonds), $L=32$ (squares), $L=48$ (stars), and $L=64$ (circles).

$$S(\vec{k}) = \langle |M(\vec{k})|^2 \rangle, \quad M(\vec{k}) = \frac{1}{L} \sum_i \sigma_i e^{i\vec{k} \cdot \vec{r}_i} \quad (13)$$

vs $\vec{k}=(k_x, k_y)$ was evaluated to check whether the wave vector of the striped configuration changes with temperature.

In Fig. 1 we show the specific heat, the staggered magnetization, the staggered susceptibility, and the fourth order energy cumulant for $J/g=0$ (AF phase). The finite-size scaling of all these quantities about $k_B T/g \approx 2.4$ points out the existence of a continuous phase transition. In particular, the fourth order energy cumulant V_L is expected to show a sharp minimum in correspondence of a first order phase transition and to be flat when the transition is continuous.¹⁵ As one can see from Fig. 1(d) V_L shows a minimum for small lattices becoming less pronounced as the lattice size increases, disappearing for lattices of a size greater than 64. In a first order phase transition¹⁵ the maximum of the specific heat and of the staggered susceptibility is expected to diverge as L^d ($d=2$ in the present case). The finite-size scaling shown in Figs. 1(a) and 1(c) indicates a much weaker divergence.

Assuming that the transition is continuous, in order to get an insight into the critical behavior of the model we look for the functions $Y^0(x)$ and $X^0(x)$ for the staggered susceptibility and for the order parameter. As one can see from Figs. 2(a) and 2(b) the MC data points for different lattice size ($L=16, 32, 48, 64$) fall on the universal curves $Y^0(x)$ and $X^0(x)$ as predicted by the finite-size scaling theory [Eq. (11)] and a straight line behavior is found in the log-log plot for large x according to Eq. (12). The critical temperature ob-

tained by the fitting is $k_B T_c/g = 2.37 \pm 0.01$, in good agreement with the critical temperature estimated by MacIsaac *et al.*¹⁰ $k_B T_c/g = 2.39 \pm 0.05$ obtained by extrapolation to $L \rightarrow \infty$ of the plot of $T_c(L)$ vs $1/L$. As for the critical exponents we find $\gamma = \gamma' = 1.75 \pm 0.02$, $\nu = 1.0 \pm 0.02$, $\beta = 0.125 \pm 0.005$ that coincide with those of the 2D NN Ising model and agree with $\beta/\nu = 0.14 \pm 0.1$ and $\gamma/\nu = 1.8 \pm 0.1$ obtained from a previous MC simulation.¹⁰ The critical amplitudes obtained from Fig. 2(a) are $C^+ = 0.39$ and $C^- = 0.017$. From Fig. 2(b) we obtain $B = 1.22$. In this figure it is also shown the universal function for $T > T_c$ expected to show the asymptotic behavior¹⁸ $X^+(x) \rightarrow B^+ x^{-\nu+\beta}$ for large x . As for the maximum of the specific heat [Fig. 1(a)] a least-square fit of the MC data with the function $C_{\max} = A_0 \ln L + B_{\max}$ leads to $A_0 = 0.55 \pm 0.01$, $B_{\max} = 0.05 \pm 0.03$. Note that for the 2D NN Ising model the exact values¹⁹ of A_0 and B_{\max} are $A_0 = 0.4945386$, $B_{\max} = 0.201359$. Incidentally, our MC simulations performed for $J/g \rightarrow \infty$ (NN Ising model) give $A_0 = 0.493 \pm 0.008$, $B_{\max} = 0.20 \pm 0.03$, a result that gives credence to our MC simulation.

In Fig. 3 we show the finite-size scaling of C , χ_{st} , m_{st} , V_L for $J/g=1.7$ ($h=1$). The divergence of the maximum of both specific heat and staggered susceptibility together with the vanishing of the minimum in the fourth order energy cumulant for large L entitle us to believe that the transition is still continuous. To investigate the critical behavior in more detail we try to fit MC data for χ_{st} and m_{st} with universal functions as given by Eq. (11). As shown in Fig. 4 the universal behavior is obtained for $k_B T_c/g = 0.82$, $\gamma = \gamma' = 1.75 \pm 0.05$, $\nu = 1.0 \pm 0.05$, and $\beta = 0.08 \pm 0.01$. Note the linear behavior of

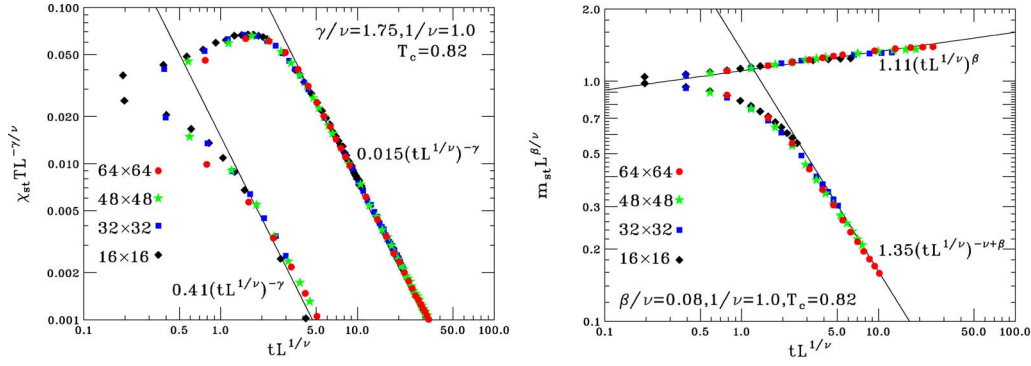


FIG. 4. (Color online) Finite-size scaling functions for $J/g=1.7$: (a) staggered susceptibility χ_{st} , (b) staggered magnetization m_{st} for $L=16$ (diamonds), $L=32$ (squares), $L=48$ (stars), and $L=64$ (circles).

$Y^0(x)$ and $X^0(x)$ at large x in the log-log plot. The critical exponents γ and ν coincide with those of the 2D NN Ising model. On the other hand, β differs from the Ising value $\beta=0.125$ outside the error uncertainty.

The scaling law $\alpha=2-2\beta-\gamma$ suggests a value of the specific heat critical exponent $\alpha=0.09\pm 0.07$. In Fig. 5(a) we give the universal function for the specific heat assuming $\alpha=0.09$, $\nu=1$, and $k_B T_c/g=0.82$ as obtained from the finite-size scaling analysis of the susceptibility and of the order parameter. Because of the very weak divergence of the specific heat at the transition, a background has to be subtracted in order to single out the singular part of the specific heat.¹⁸ A satisfactory universal behavior is obtained for a background value $B_g=-5.3$. Note that even the hyperscaling law $d\nu=2-\alpha$ is satisfied within the error bars.

An interesting check can be done about the critical behavior of the order parameter¹⁶ O_{hw} [Eq. (5)], which is particularly convenient for the striped configurations, and the staggered magnetization m_{st} [Eq. (7)]. The temperature dependence of O_{hw} is very similar to that of m_{st} shown in Fig. 3(b). As shown in Fig. 5(b) even the critical behavior is quite similar. The critical temperature and the critical exponents for O_{hw} are the same as those deduced from the universal function for m_{st} . Only the critical amplitudes differ somewhat as can be seen comparing Figs. 4(b) and 5(b) but it is well known that the critical amplitudes are not universal.

This is an interesting point: for striped configurations two different thermodynamic quantities as O_{hw} and the staggered

magnetization m_{st} can be chosen as order parameter. Indeed both are different from zero in the ordered phase ($T < T_c$) and vanish in the paramagnetic phase ($T > T_c$). However, the nonuniversal choice of the order parameter does not change the universal character of a continuous phase transition.

In Fig. 6 we show the structure factor [Eq. (13)] for $J/g=1.7$. A single MC run of 10^5 MCS is performed for each temperature shown. The lattice chosen for the simulation is a square lattice of edge $L=64$ so that the finite Fourier transform wave vectors are $\vec{k}=2\pi/64(Q_x, Q_y)$ where $Q_x, Q_y = -31, -30, \dots, 0, \dots, 32$ corresponding to $-\pi < k_x, k_y \leq \pi$. We have obtained the structure factor for several temperatures. From $T=0$ to $k_B T/g=0.80$ [see Fig. 6(a)] the structure factor has a single peak at $\vec{k}=(\pi, 0)$ corresponding to columns of parallel spins that alternate moving along a row: $\langle 1 \rangle$ phase. The intensity of the peak decreases very slowly moving from the saturation value $S(\pi, 0)/L^2=1$ at $T=0$ as the temperature increases. Close to the critical temperature $k_B T_c/g=0.82$ the drop is very sharp: the height of the peak is 0.922, 0.853, 0.691 at $k_B T/g=0.70, 0.75, 0.80$, respectively. Above T_c a symmetric peak at $\vec{k}=(0, \pi)$ appears as shown in Fig. 6(b) for $k_B T/g=0.83$, indicating that the system can move freely from vertical to horizontal stripes. For temperatures slightly above T_c the peaks become very weak (0.06 at $k_B T/g=0.86, 0.02$ at $k_B T/g=0.89$) but their location does not change.

In Fig. 7 we show the finite-size scaling of the specific heat C , the order parameter O_{hw} , the energy per spin E/g , and

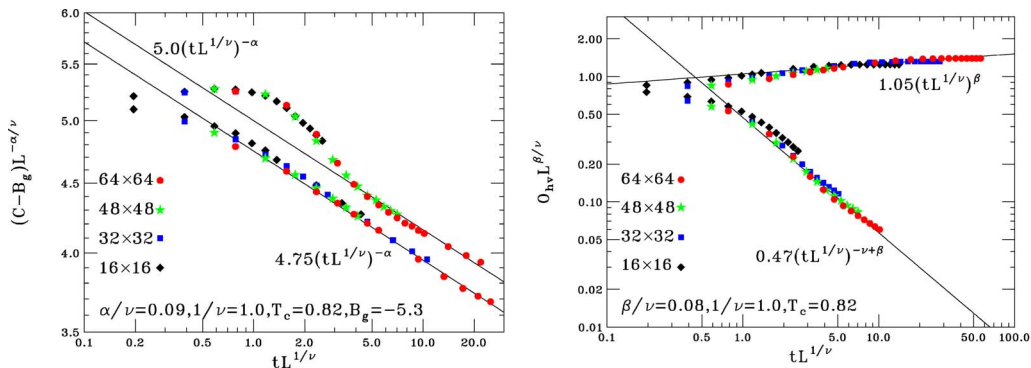


FIG. 5. (Color online) Finite-size scaling functions for $J/g=1.7$: (a) specific heat, (b) order parameter O_{hw} for $L=16$ (diamonds), $L=32$ (squares), $L=48$ (stars), and $L=64$ (circles).

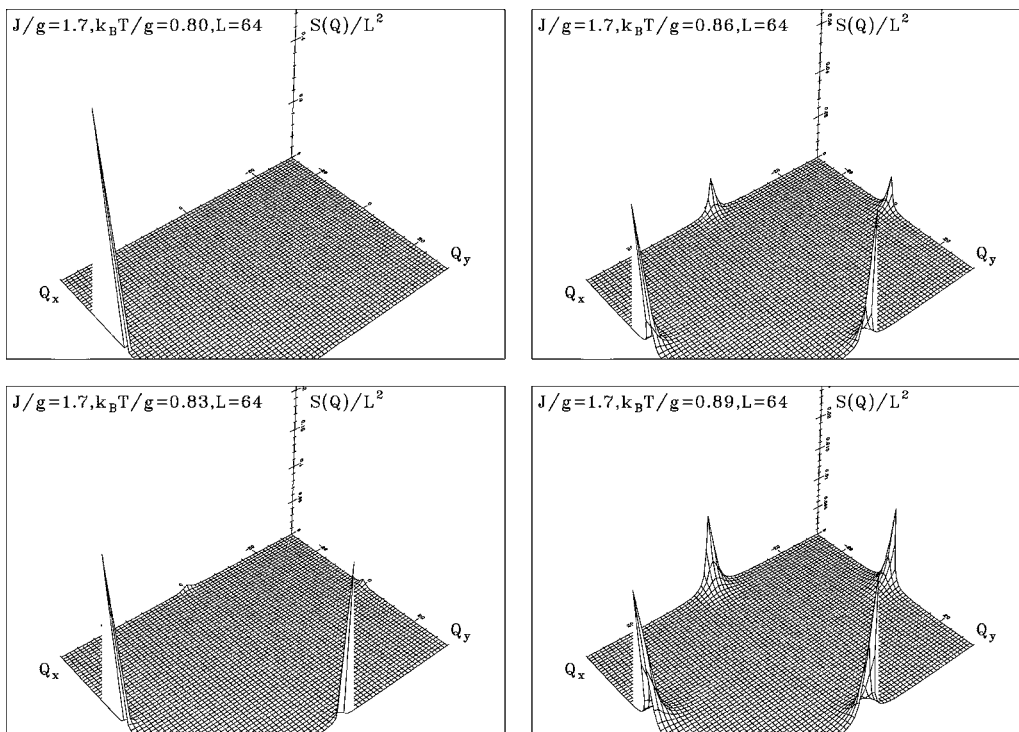


FIG. 6. Structure factor vs wave vector for $J/g=1.7$ and $L=64$ at (a) $k_B T/g=0.80$, (b) 0.83 (T_c), (c) 0.86 , and (d) 0.89 .

the fourth order energy cumulant V_L for $J/g=3.4$ ($h=2$). As one can see in Fig. 7(a) the maximum of the specific heat diverges as $L \rightarrow \infty$ with a power lesser than but not far from 2. For instance, $C(64)/C(48) \approx 1.67 = (64/48)^d$ with d

$= 1.8 \pm 0.2$. The order parameter O_{hw} shows a steep drop about T_c at increasing lattice size L as shown in Fig. 7(b). Any attempt to find a universal function $X^0(x)$ failed. The internal energy seems to point out a discontinuity as L in-

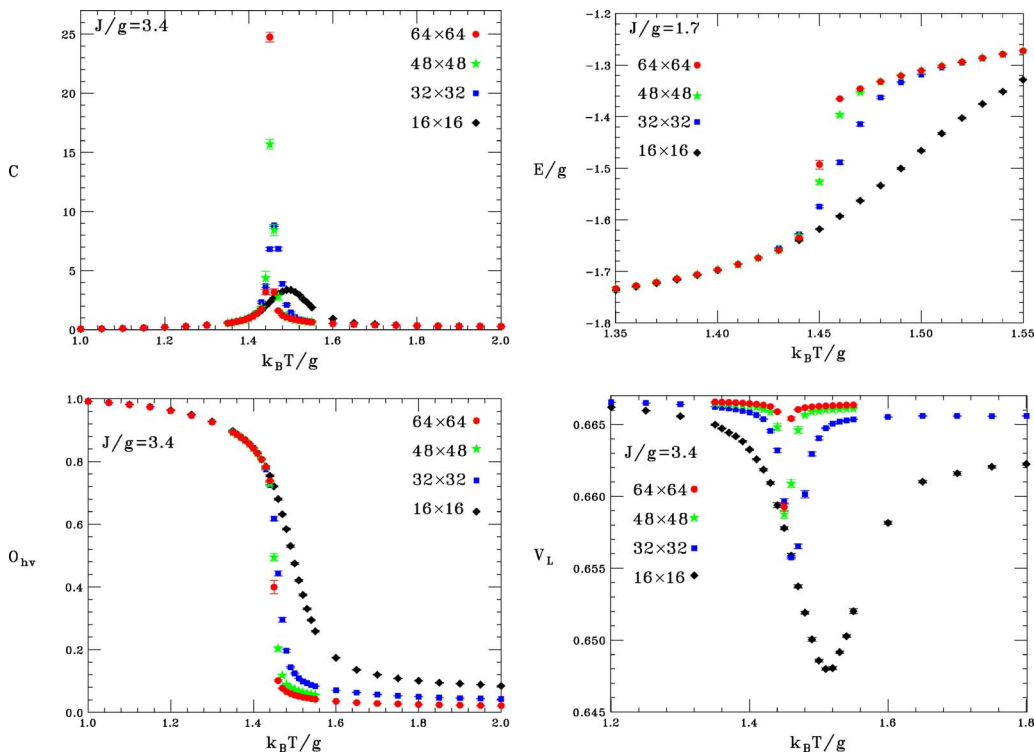


FIG. 7. (Color online) Thermodynamic quantities for $J/g=3.4$ ($h=2$): (a) specific heat, (b) order parameter, (c) internal energy, (d) fourth order energy cumulant vs temperature for $L=16$ (diamonds), $L=32$ (squares), $L=48$ (stars), and $L=64$ (circles).

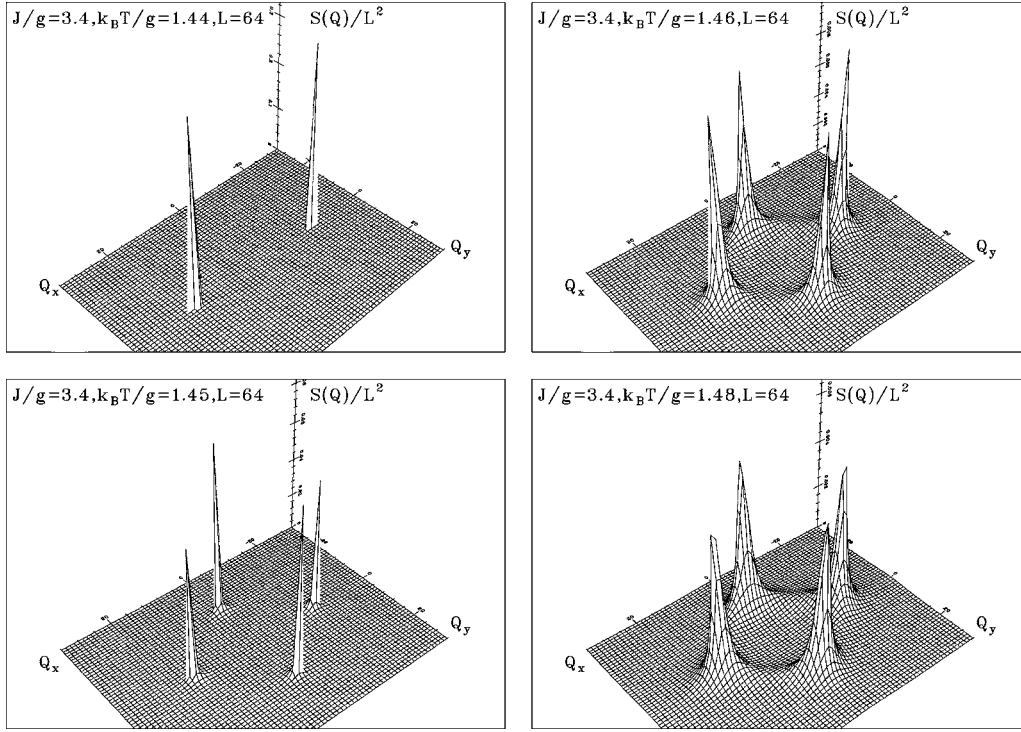


FIG. 8. Structure factor vs wave vector for $J/g=3.4$ and $L=64$ at (a) $k_B T/g=1.44$, (b) 1.45 (T_c), (c) 1.46 , and (d) 1.48 .

creases as shown in Fig. 7(c). Finally, V_L shows a deep minimum even for the largest lattice size $L=64$. Note that the minimum of the fourth order energy cumulant V_m for the infinite-lattice model at T_c is given by¹⁵

$$V_m = 1 - \frac{(E_-^2 + E_+^2)^2}{12E_-^2 E_+^2}, \quad (14)$$

where E_{\pm} are the energies of the high temperature paramagnetic (+) and low temperature ordered (-) phase that coexist at the transition. We have performed a MC run at $k_B T_c/g = 1.45$ in order to obtain the energy density distribution $D(E)$. A two-peak structure is found and we have fitted $D(E)$ by the sum of two Gaussians

$$D(E) = \frac{A_-}{\sigma_- \sqrt{2\pi}} e^{-(E-E_-)^2/2\sigma_-^2} + \frac{A_+}{\sigma_+ \sqrt{2\pi}} e^{-(E-E_+)^2/2\sigma_+^2}, \quad (15)$$

obtaining $E_-/g = -1.603 \pm 0.004$, $\sigma_- = 0.061 \pm 0.004$, $A_- = 0.45 \pm 0.02$, and $E_+/g = -1.384 \pm 0.001$, $\sigma_+ = 0.072 \pm 0.001$, $A_+ = 0.57 \pm 0.02$. Inserting these data in Eq. (14) and evaluating the error in the standard way

$$\Delta V_m = \sqrt{\left(\frac{\partial V_m}{\partial E_-}\right)^2 (\Delta E_-)^2 + \left(\frac{\partial V_m}{\partial E_+}\right)^2 (\Delta E_+)^2}, \quad (16)$$

we obtain

$$V_m = 0.6594 \pm 0.0003, \quad (17)$$

which compares very well with the value deduced by MC data for $L=64$. Indeed from Fig. 7(d) one has

$$V_m(L=64) = 0.6593 \pm 0.0003. \quad (18)$$

For all these reasons we conclude that the transition is first order.

In Fig. 8 we give the structure factor for a lattice with $L=64$ at several temperatures around $k_B T_c/g=1.45$. The location of the peaks is $\vec{k}=(\pm\pi/2, 0)$ corresponding to the $\langle 2 \rangle$ phase characterized by vertical stripes of width $h=2$. The intensity of each peak is $1/2$ at $T=0$ and moves from the saturation value very slowly: indeed the intensity is $0.497, 0.436, 0.418, 0.381$ at $k_B T/g=1, 1.40, 1.42, 1.44$, respectively. At the transition temperature four peaks of intensity ~ 0.07 located at the symmetric positions $\vec{k}=(\pm\pi/2, \pm\pi/2)$ occur reflecting the free motion of the stripes. In order to enlighten on the dynamics of the stripes during the MC evolution we show in Fig. 9 some snapshots of the lattice configurations representative of the hundreds taken during the MC run. The structure factor of Fig. 8(b) is the average over the 10^4 instantaneous configurations (out of 10^5 MCS) of which the snapshots of Fig. 9 are a sample. Figure 9(a) shows horizontal stripes with $S(0, \pi/2)/L^2 \approx 0.36$, $S(\pi/2, 0)/L^2 \approx 0$, $n_h - n_v / n_h + n_v \approx -0.68$ and energy per spin $E/g = -1.61$. Figure 9(b) shows a mixing of horizontal and vertical stripes (tetragonal¹⁶ phase) with $S(0, \pi/2)/L^2 \approx S(\pi/2, 0)/L^2 \approx 0$, $n_h - n_v / n_h + n_v \approx -0.15$ and energy per spin $E/g = -1.39$. Figure 9(c) shows vertical stripes configurations with $S(0, \pi/2)/L^2 \approx 0$, $S(\pi/2, 0)/L^2 \approx 0.39$, $n_h - n_v / n_h + n_v \approx 0.76$ and energy per spin $E/g = -1.66$. Note that the values of the energy per spin of the striped configurations and of the tetragonal one correspond to the jump observed at $T=T_c$ in Fig. 7(c). Also the values of the order parameter O_{hv} in the striped configuration (~ 0.7) and in the

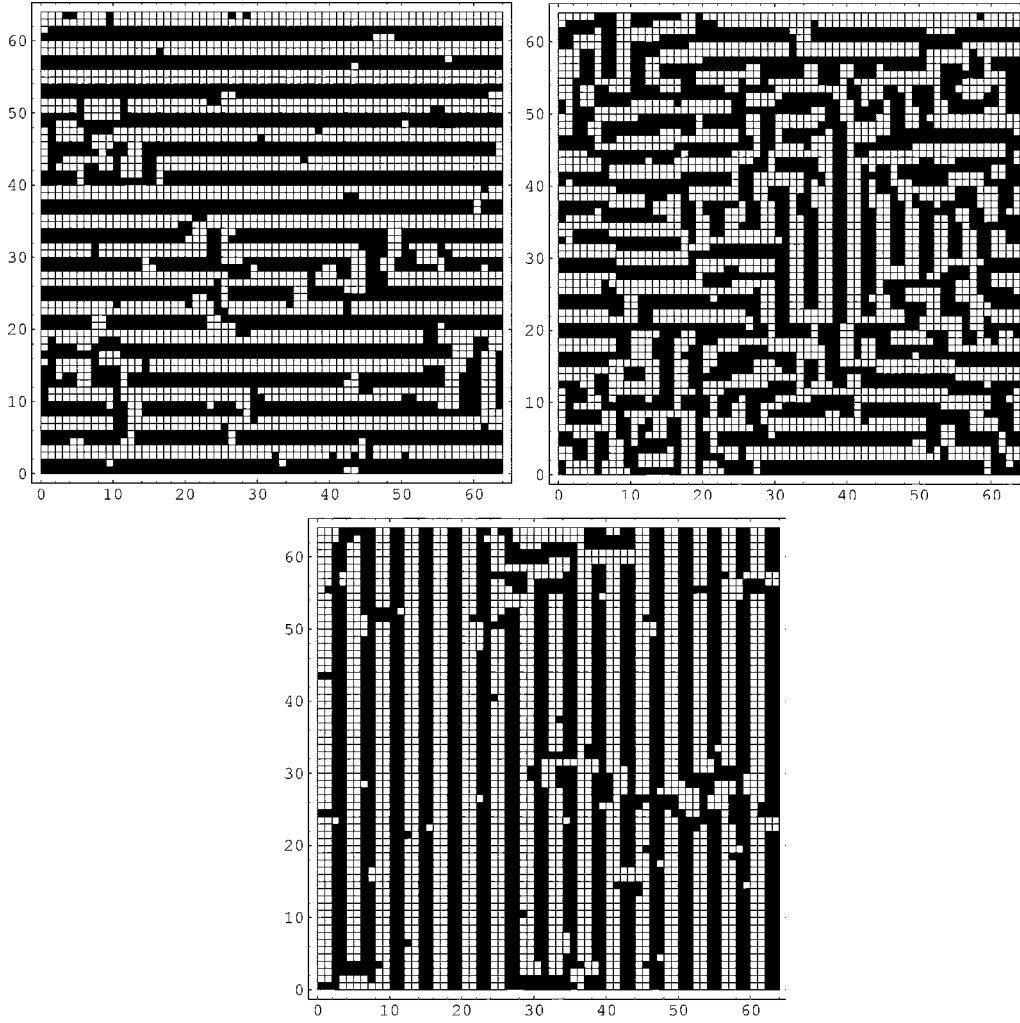


FIG. 9. Snapshots for $J/g=3.4$ and $L=64$ at $k_B T_c/g=1.45$. White and black squares represent spin up and down, respectively.

tetragonal one (~ 0.15) correspond to the jump shown in Fig. 7(b). In Fig. 8(d) at $k_B T_c/g=1.48$ a crown appears connecting the four symmetric peaks dramatically reduced in intensity (0.006). In conclusion, for $J/g=3.4$ ($h=2$) we obtain a scenario in agreement with Cannas *et al.*,¹¹ that is a strong indication of a first order phase transition.

In Fig. 10 we show the finite-size scaling of the specific heat C , the order parameter O_{hw} , the energy per spin E/g , and the fourth order energy cumulant V_L for $J/g=5$ ($h=3$). As one can see in Fig. 10(a) the maximum of the specific heat diverges as $L \rightarrow \infty$ with a power between 1 and 2. For instance, $C(96)/C(48) \approx 2.25 \pm 0.13 = 2^d$ with $d=1.17 \pm 0.08$. This value is certainly far from 2, however, it is larger than the critical exponent of any known continuous transition. The order parameter O_{hw} shows a steep decrease at T_c [Fig. 10(b)]. On the other hand, no jump at T_c occurs in the internal energy versus T even for the largest lattice size ($L=96$) [Fig. 10(c)]. The fourth order energy cumulant V_L shows a deep minimum that survives even for $L=96$ [Fig. 10(d)]. These conflicting results lead us to believe that the transition is weakly first order in agreement with the expectation of Cannas *et al.*¹¹

In Fig. 11 we give the structure factor for $J/g=5$ obtained by a MC simulation performed on a lattice of size $L=96$ at

several temperatures around $k_B T_c/g=2.12$. The peaks are located at $\vec{k}=(\pm\pi/3, 0)$ (main peaks) and $(\pi, 0)$ corresponding to the $\langle 3 \rangle$ phase characterized by vertical stripes of width $h=3$. At $T=0$ the intensity of the two main peaks is $4/9$ and that of the lower peak is $1/9$. At $k_B T/g=2.10$ the intensities become 0.310 and 0.036, respectively. The peak at $(\pi, 0)$ has an intensity about $1/10$ of that of the peaks at $(\pm\pi/3, 0)$ while at $T=0$ the ratio is $1/4$. At the critical temperature the peak at $(\pi, 0)$ disappears and four peaks located at $(\pm\pi/3, \pm\pi/3)$ occur, the intensity of which is between 0.02 and 0.05.

In Fig. 12 we show the finite-size scaling of the specific heat C , the order parameter O_{hw} , the energy per spin E/g , and the fourth order energy cumulant V_L for $J/g=6$ ($h=4$). The maximum of the specific heat [Fig. 12(a)] increases as L^d with $d \leq 2$. For instance $C(64)/C(48) \approx 1.2 \pm 0.1 = (4/3)^d$ with $d=0.6 \pm 0.3$. The smoothness of the order parameter [Fig. 12(b)] and of the energy per spin [Fig. 12(c)] together with the vanishing of the minimum in the fourth order energy cumulant [Fig. 12(d)] at increasing L leads us to conclude that the transition is continuous.

In Fig. 13 we give the structure factor for a lattice with $L=64$ at several temperatures around $k_B T_c/g=2.71$. At $T=0$

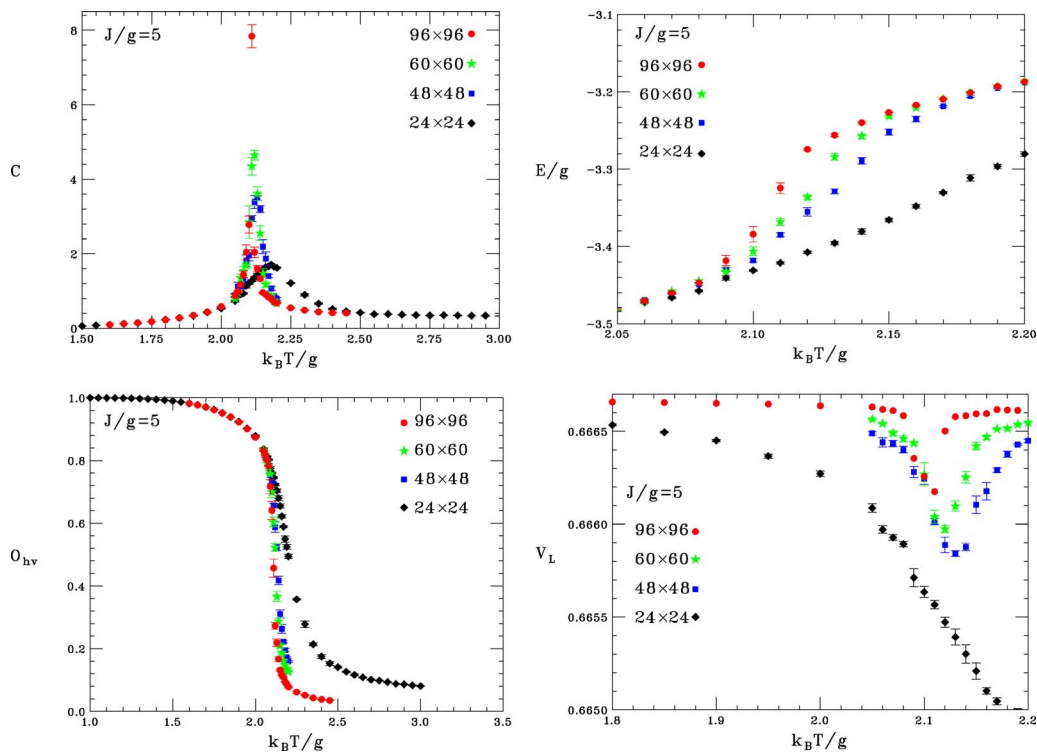


FIG. 10. (Color online) Thermodynamic quantities for $J/g=5$ ($h=3$): (a) specific heat, (b) order parameter, (c) internal energy, (d) fourth order energy cumulant vs temperature for $L=24$ (diamonds), $L=48$ (squares), $L=60$ (stars), and $L=96$ (circles).

the peaks are located at $\vec{k}=(\pm\pi/4,0)$ and $(\pm3\pi/4,0)$ with intensity $(2+\sqrt{2})/2=0.4268$ and $(2-\sqrt{2})/2=0.0732$, respectively. These peaks correspond to the $\langle 4 \rangle$ phase characterized by vertical stripes of width $h=4$. At $k_B T/g=2.69$ [Fig. 13(a)]

the intensity of the higher peaks reduce to 0.226 and the lower peaks disappear in the background. At the critical temperature a four-peak structure occurs with symmetric peaks located at $(\pm\pi/4, \pm\pi/4)$ with an intensity that drops very

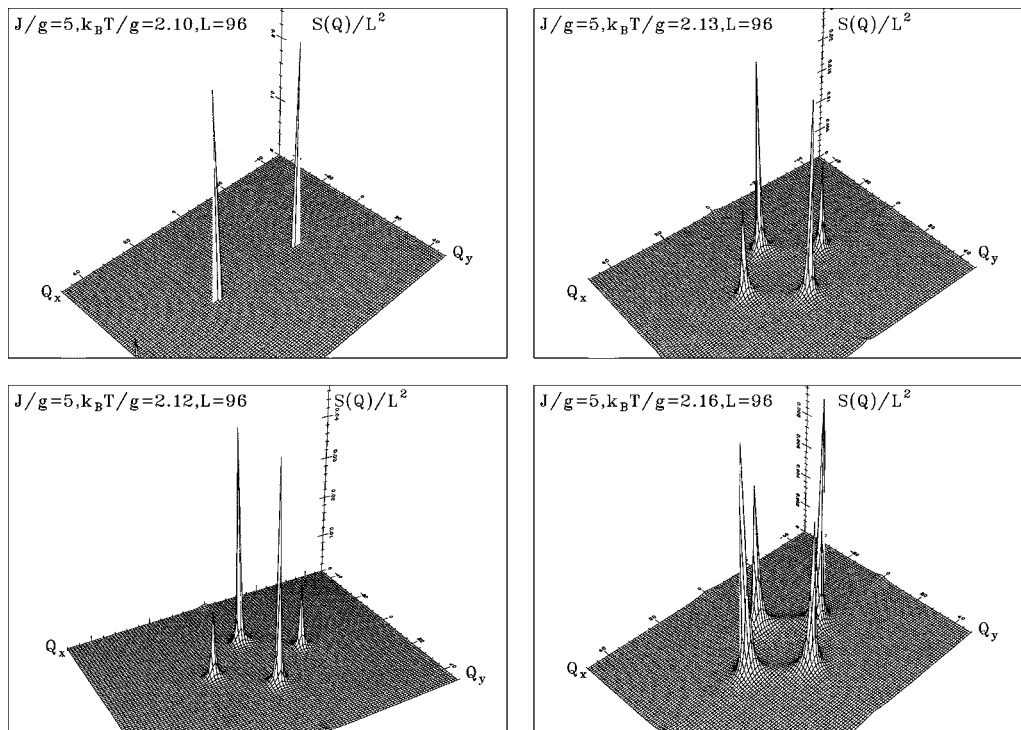


FIG. 11. Structure factor vs wave vector for $J/g=5$ ($h=3$) and $L=96$ at (a) $k_B T/g=2.10$, (b) 2.12 (T_c), (c) 2.13 , and (d) 2.16 .

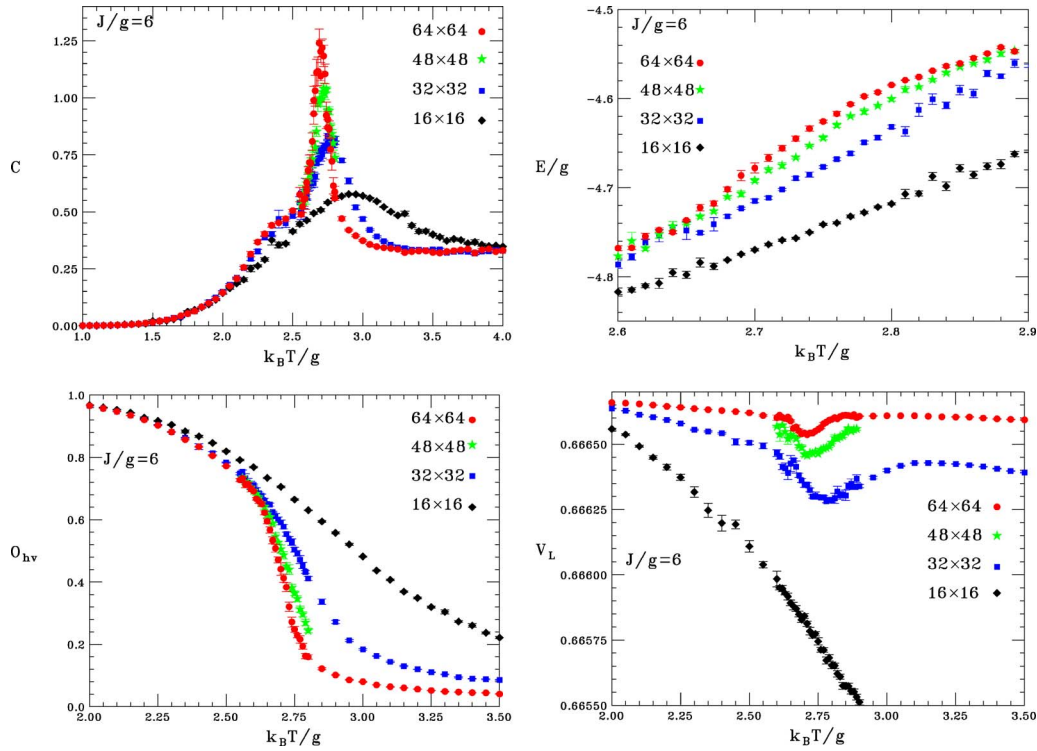


FIG. 12. (Color online) Thermodynamic quantities for $J/g=6$ ($h=4$): (a) specific heat, (b) order parameter, (c) internal energy, (d) fourth order energy cumulant vs temperature for $L=16$ (diamonds), $L=32$ (squares), $L=48$ (stars), and $L=64$ (circles).

quickly. For instance at $k_B T/g=2.77$ the main peak intensity is ~ 0.02 .

The finite-size scaling analysis of O_{hv} is consistent with $\beta=1/8$ and $\nu=1$ with $k_B T_c/g=2.71$. Even the maximum of

the specific heat is consistent with the logarithmic behavior $C_m=A_0 \ln L+B_{max}$ with $A_0=0.48\pm 0.04$ and $B_{max}=-0.80\pm 0.17$. The scenario is undistinguishable from that of the 2D NN Ising model. Note that for $J/g\rightarrow\infty$ we recover

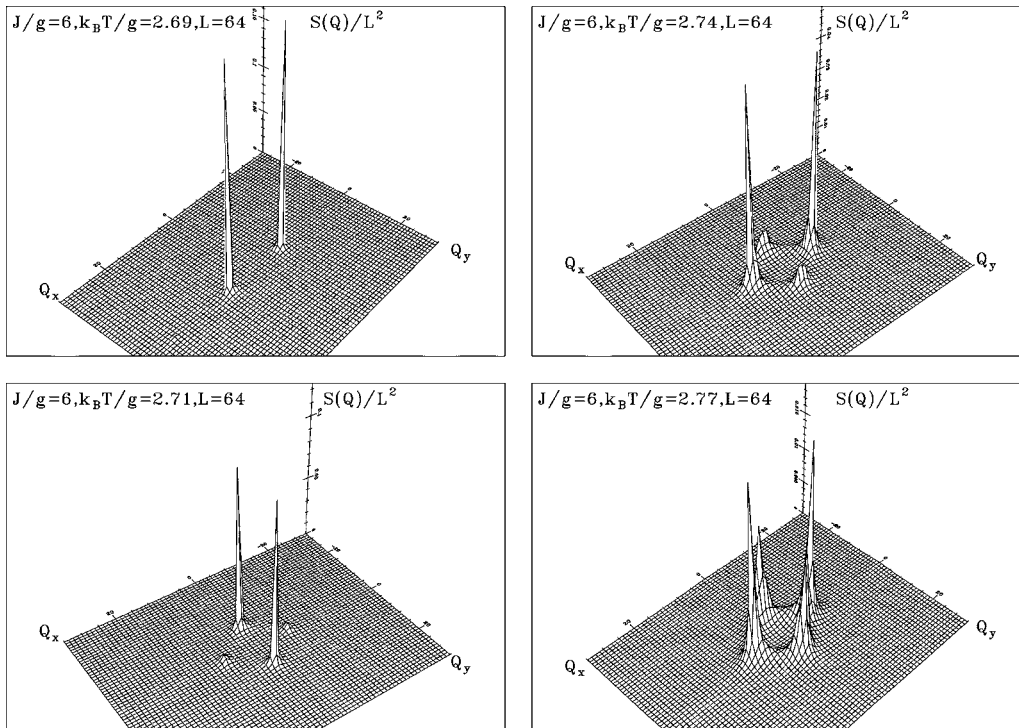


FIG. 13. Structure factor vs wave vector for $J/g=6$ and $L=64$ at (a) $k_B T/g=2.69$, (b) 2.71 (T_c), (c) 2.74 , and (d) 2.77 .

the Ising values¹⁹ $A_0=0.493\pm 0.008$ and $B_{max}=0.20\pm 0.03$.

III. CONCLUSIONS

Frustration caused by the simultaneous presence of NN ferromagnetic exchange and dipole interaction in a square Ising model gives a variety of spin configurations. Indeed for pure dipole interaction ($J=0$) the stable state corresponds to an antiferromagnetic Néel configuration while for pure exchange interaction ($g=0$) a ferromagnetic spin configuration sets up. For $J/g\neq 0$ the stable states correspond to striped configurations of h columns (rows) with spins up followed by h columns (rows) with spins down, the width h increasing as J/g increases. Continuous phase transitions of the 2D NN Ising model universality class occur for $J=0$ and for $J/g\geq 6$. For large J/g a first order transition driven by fluctuations was suggested on the basis of the self-consistent Hartree-Fock approximation¹¹ applied to a continuum version of Hamiltonian (1). However, this approximation leads to a first order phase transition even for $g=0$ (2D NN Ising

model) where the transition is certainly continuous.

The $h=1$ spin configuration undergoes a continuous order-disorder phase transition with critical exponents out of any known universality class. Indeed we find $\beta=0.08$, $\gamma=1.75$, $\nu=1$, and $\alpha=0.09$ by a careful finite-size scaling analysis of MC data. A first order phase transition for the $h=2$ striped configuration is unambiguously recognized, while a weakly discontinuous phase transition is suggested in $h=3$ striped configuration. In all MC simulations we have performed no change of the wave vector characterizing the spin configuration at increasing temperature was recorded and no intermediate Kosterlitz-Thouless phase between the low temperature ordered phase and the paramagnetic one was singled out in contrast with the behavior of the 3D and 2D ANNNI model.¹

ACKNOWLEDGMENTS

We would like to thank the staff of the Advanced Calculation Laboratory (LCA) of the Physics Department of the University of Parma and, in particular, Fabio Spataro.

*Present address: Istituto IMEM of CNR, Parco Area delle Scienze, 43100 Parma, Italy; electronic address: rastelli@fis.unipr.it

¹W. Selke, Phys. Rep. **170**, 213 (1988).

²W. Selke and M. E. Fisher, Phys. Rev. B **20**, 257 (1979).

³J. Villain and P. Bak, J. Physique **42**, 657 (1981).

⁴W. Selke, Z. Phys. B: Condens. Matter **43**, 335 (1981).

⁵K. Binder and D. P. Landau, Phys. Rev. B **21**, 1941 (1980).

⁶J. V. José, L. P. Kadanoff, S. Kirkpatrick, and D. R. Nelson, Phys. Rev. B **16**, 1217 (1977).

⁷E. Rastelli, S. Regina, and A. Tassi, Phys. Rev. B **69**, 174407 (2004); **70**, 174447 (2004).

⁸A. B. MacIsaac, J. P. Whitehead, M. C. Robinson, and K. De'Bell, Phys. Rev. B **51**, 16033 (1995).

⁹K. De'Bell, A. B. MacIsaac, and J. P. Whitehead, Rev. Mod. Phys. **72**, 225 (2000).

¹⁰A. B. MacIsaac, J. P. Whitehead, K. De'Bell, and K. S. Narayanan, Phys. Rev. B **46**, 6387 (1992).

¹¹S. A. Cannas, D. A. Stariolo, and F. A. Tamarit, Phys. Rev. B **69**, 092409 (2004).

¹²S. A. Brazovskii, Zh. Eksp. Teor. Fiz. **68**, 175 (1975) [Sov. Phys. JETP **41**, 85 (1975)].

¹³M. Grousson, V. Krakoviack, G. Tarjus, and P. Viot, Phys. Rev. E **66**, 026126 (2002).

¹⁴M. B. Taylor and B. L. Gyorffy, J. Phys.: Condens. Matter **5**, 4527 (1993).

¹⁵M. S. S. Challa, D. P. Landau, and K. Binder, Phys. Rev. B **34**, 1841 (1986); A. Billoire, R. Lacaze, A. Morel, S. Gupta, A. Irbäck, and B. Petersson, *ibid.* **42**, 6743 (1990).

¹⁶I. Booth, A. B. MacIsaac, J. P. Whitehead, and K. De'Bell, Phys. Rev. Lett. **75**, 950 (1995).

¹⁷M. E. Fisher, *Proceedings of the International School "Enrico Fermi"* (Academic, New York, 1971), Course LI.

¹⁸D. P. Landau, Phys. Rev. B **13**, 2997 (1976).

¹⁹A. E. Ferdinand and M. E. Fisher, Phys. Rev. **185**, 832 (1969).